Supporting Information

Jung et al. 10.1073/pnas.1305025110

SI Text

The Capacity Contributions from Carbonaceous Components

The capacity contributions from the carbonized polydopamine and Super P were calculated on the basis of the following procedure. It should be particularly noted that the mass of Super P was not counted in the total mass of the active material following conventional capacity calculation in most reports, although it contributes to the total capacity.

- Capacity contribution of Super P in carbon-coated rice husk Si ($c\text{-}Si_{RH}$) electrode (%):

$$(\text{Weight content of Super P} \times \text{Capacity}_{\text{Super P}})/\text{Capacity}_{\text{c-SiRH}} \times 100 = (0.2 \times 170)/1,615 \times 100 = 2\%.$$

- Capacity contribution of carbonized polydopamine in $c\text{-}Si_{RH}$ (%):

$$(\text{Weight content of carbonized polydopamine in c-Si}_{RH} \times \text{Capacity}_{\text{carbonized polydopamine}})/(\text{Capacity}_{\text{c-SiRH}} - \text{Weight content of Super P} \times \text{Capacity}_{\text{Super P}}) \times 100 = (0.08 \times 196)/(1,615 - 0.2 \times 170) \times 100 = 1\%.$$

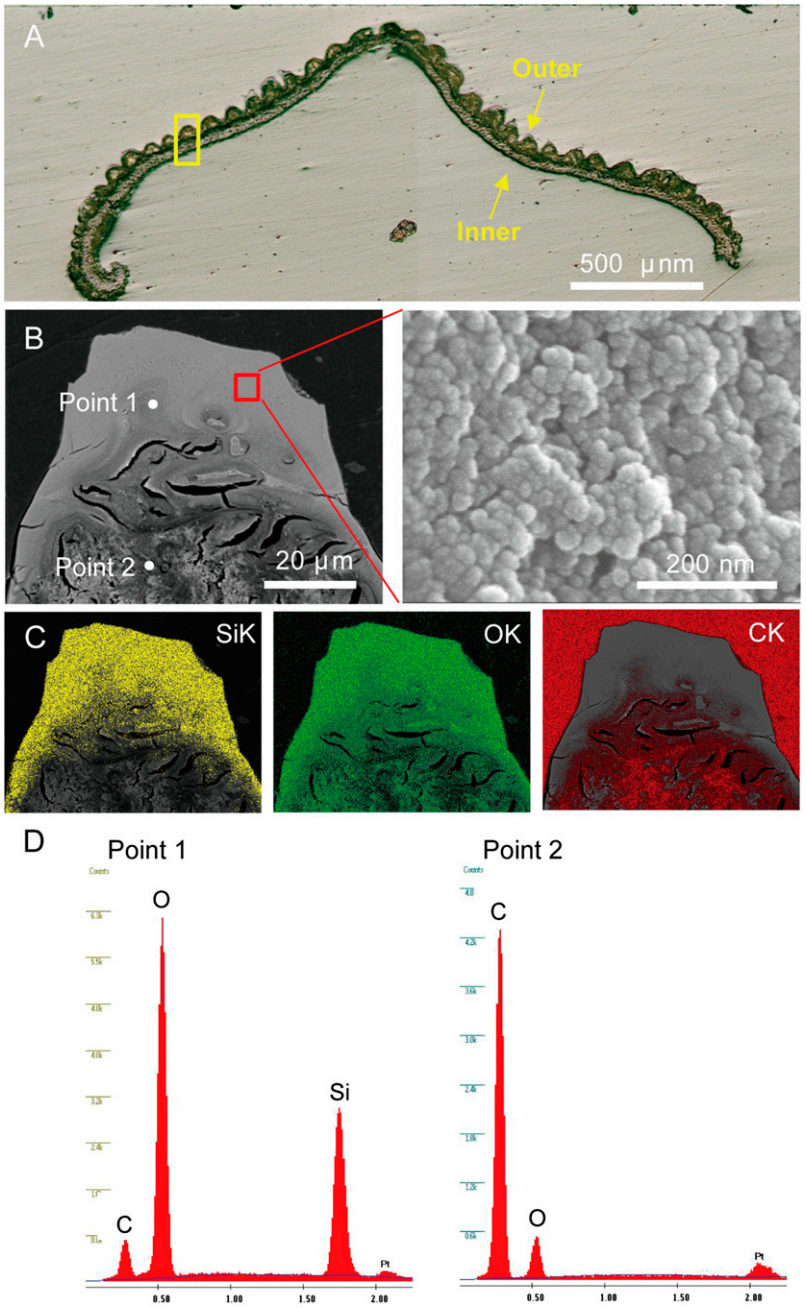

Fig. S1. (*A*) Optical microscope image of a rice husk. (*B*) (*Left*) Back-scattered electron (BSE) image of outer surface of a rice husk magnified from the yellow box in *A*. (*Right*) Field emission scanning electron microscope image of the outer rugged surface of a rice husk, indicating the silica body in the RH has a nanoporous structure. (*C*) (*Left* to *Right*) Energy-dispersive elemental mapping analyses of silicon, oxygen, and carbon, indicating that Si exists mainly along the outer surface. (*D*) Energy-dispersive X-ray spectra from points 1 and 2 in *B*.

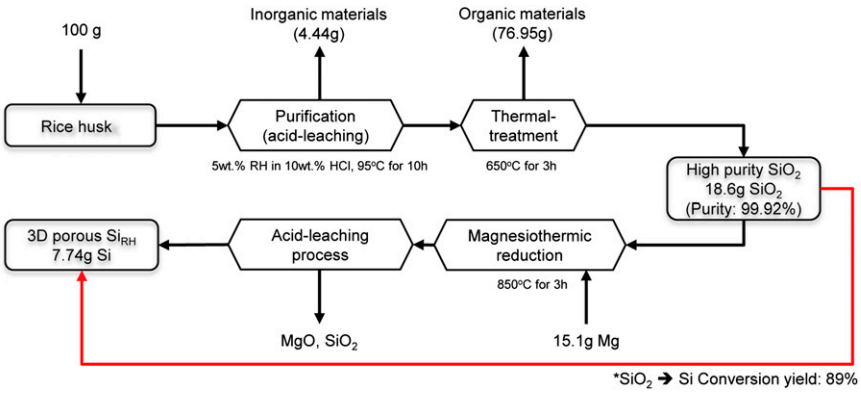

Fig. S2. Flowchart summarizing the synthetic procedures to obtain Si_{RH} from original rice husks.

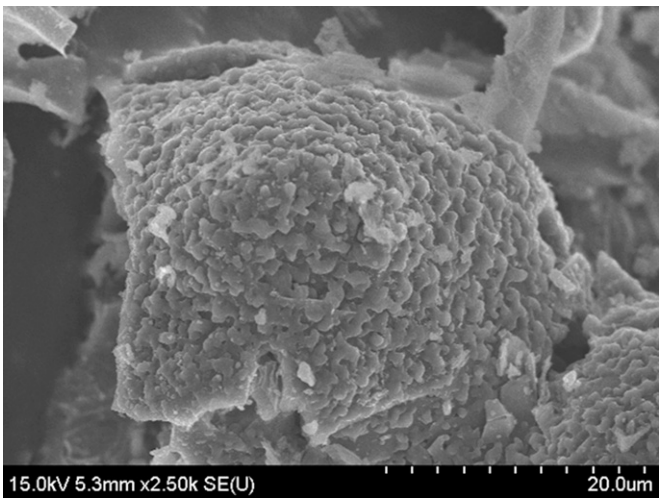

Fig. S3. SEM image of the RH-originated silicon obtained from the same synthetic procedure but with no acid treatment, indicating that the original nanoporous structure collapses if the acid treatment is omitted.

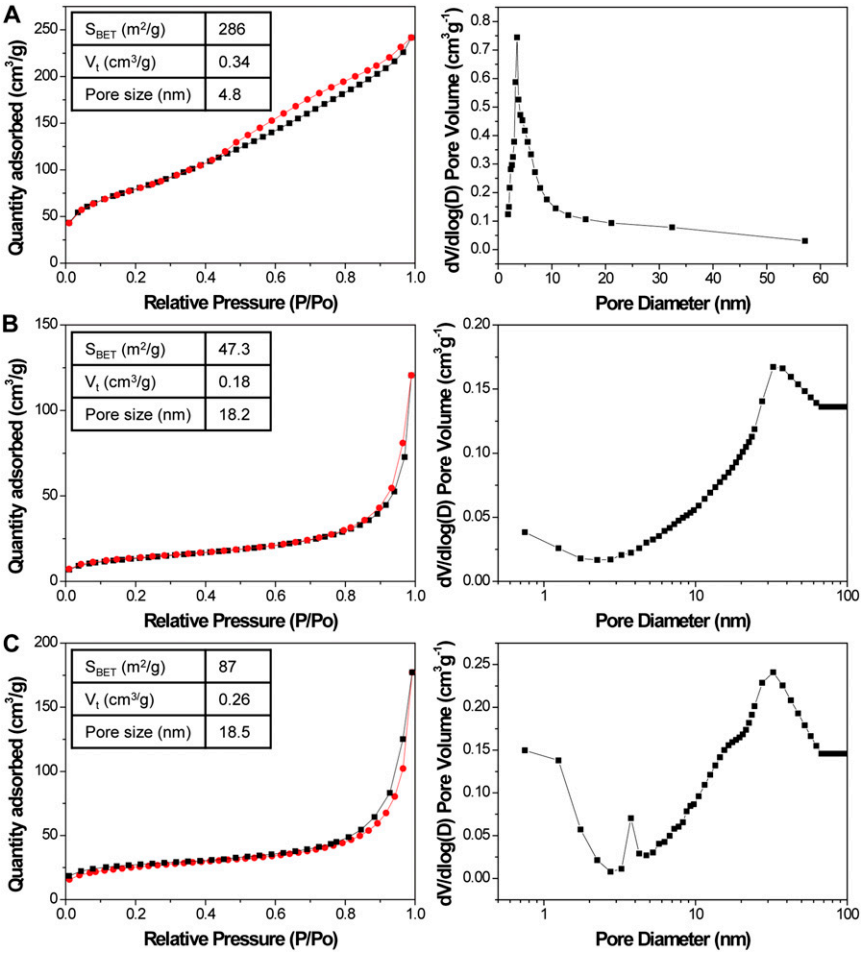

Fig. S4. Nitrogen adsorption and desorption isotherms and pore size distributions of (*A*) the rice husk-originated silica, (*B*) the rice husk-originated 3D porous silicon, and (*C*) the carbon-coated 3D porous silicon.

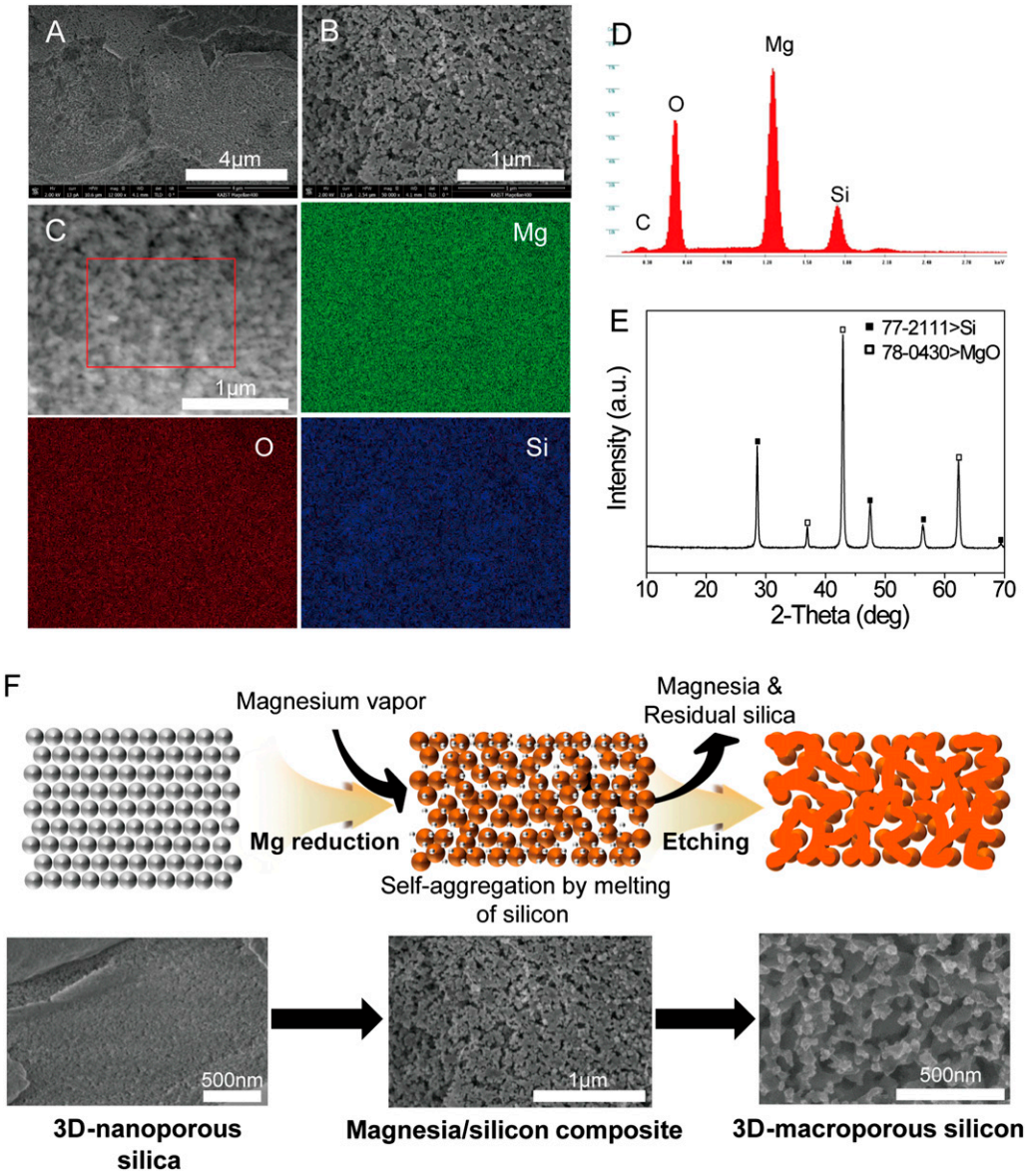

Fig. S5. (*A*) SEM image of MgO/Si mixture. (*B*) Magnified SEM image of the sample in *A*. (*C*) BSE image of MgO/Si mixture together with corresponding energy-dispersive elemental mapping analyses of magnesium, oxygen, and silicon showing homogeneous distribution of each element over the mixture particles. (*D*) Energy-dispersive X-ray spectrum obtained for the red box in *C*. (*E*) XRD pattern of the mixture, revealing the formation of silicon and magnesia after the magnesiothermic reduction. (*F*) Schematic diagram of fabrication procedure to generate 3D porous silicon from the rice husk-originated nanoporous silica by a thermally controlled magnesiothermic reduction process.

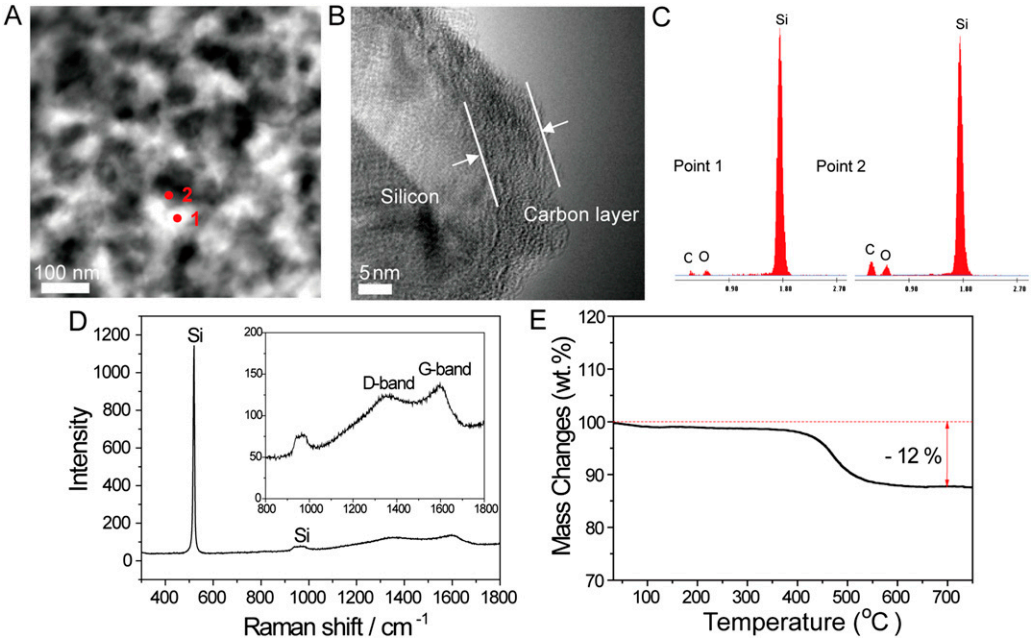

Fig. S6. Characterization of carbon-coated 3D nanoporous rice husk-originated Si (c-Si_{RH}). (*A* and *B*) STEM and HRTEM images of c-Si_{RH} revealing the preserved interconnected 3D-porous structure after the carbon coating. (*C*) Energy-dispersive X-ray spectra from points 1 and 2 in *A*. (*D* and *E*) Raman spectrum (*D*) and thermogravimetric analysis (TGA) curve (*E*) of c-Si_{RH}.

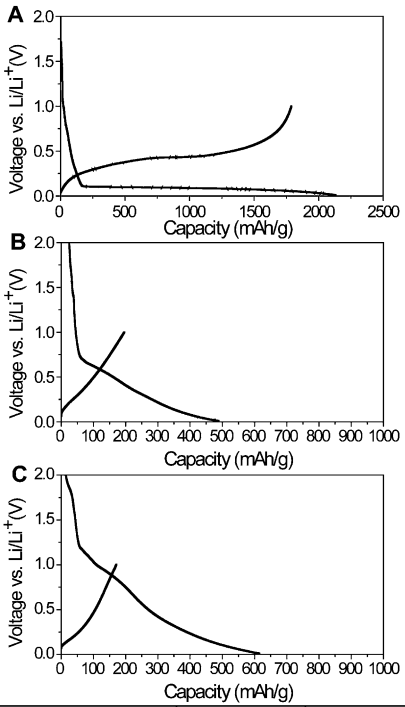

	Charge capacity (mAh/g)	Discharge capacity (mAh/g)	Coulombic efficiency (%)
Carbonized polydopamine	488.42	195.65	40
Super P	614.98	170.76	28
Rice husk originated Si (Si_{RH})	2132	1788.8	83.9
c-Si_{RH}	1918	1615	84.2

Fig. S7. (*A–C*) The first galvanostatic profiles of (*A*) Si_{RH}, (*B*) carbonized polydopamine, and (*C*) Super P with detailed specific capacities and coulombic efficiencies denoted (*C*, *Lower*).

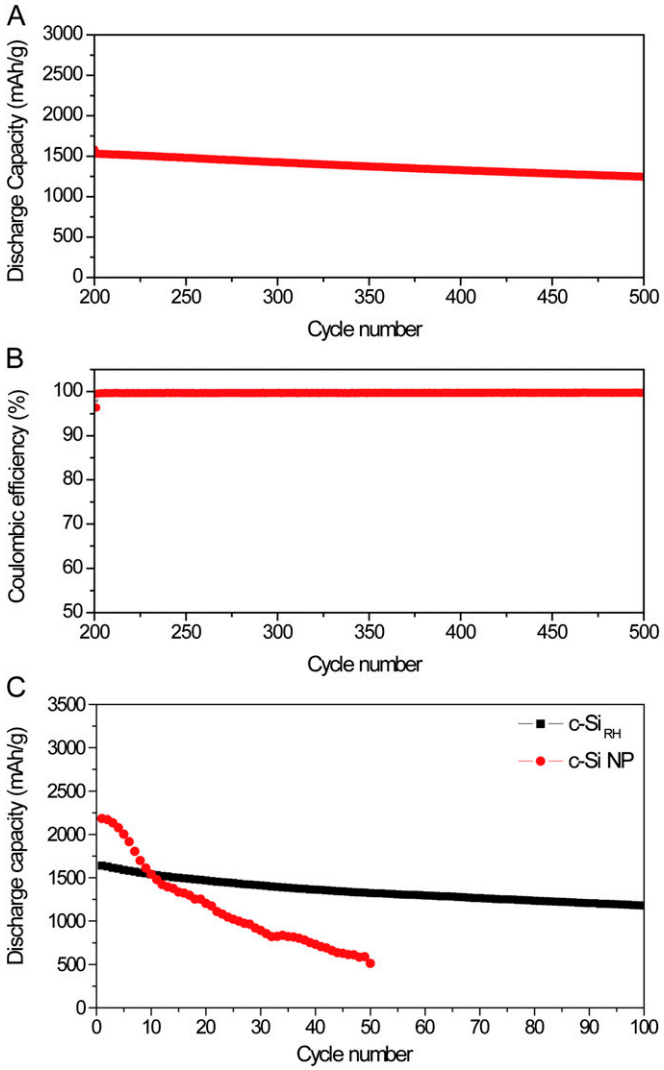

Fig. S8. (*A* and *B*) Delithiation capacities (*A*) and CEs (*B*) of c-Si_{RH} at a current rate of 6 A/g (= 3 C) during the extended 300 cycles. The data during the first 200 cycles are shown in Fig. 4*C* in the main text. (*C*) Delithiation capacities of c-Si_{RH} and c-Si nanoparticles (NPs), evaluated when the mass loadings of both electrodes increase by five times to ~1.5 mg/cm^2. Both charge and discharge were measured at a rate of 2 A/g (= 1 C).

Table S1. Contents of metallic ingredients in wt% for RHs after the heat treatment

Element	Bare RHS, μg/g
Al	282.75
B	12.4
Ba	46.18
Ca	7,942.5
Co	ND
Cr	17.91
K	31,347.79
La	ND
Li	ND
Mn	2,448.63
Na	799.25
Ni	ND
P	ND
Sr	26.39
Ti	20.74
V	ND
Zn	166.82
Zr	ND
Mg	2,079.17
Sum	45,190.53
Purity, %	95.48

The analysis indicates that the purity of the RH-originated silica obtained with no acid-treatment is 95.48%.